

Superconductivity in strongly repulsive fermions: the role of kinetic-energy frustration

L. Isaev¹, G. Ortiz¹, and C. D. Batista²

¹*Department of Physics, Indiana University, Bloomington IN 47405*

²*Theoretical Division, Los Alamos National Laboratory, Los Alamos NM 87545*

We discuss a physical mechanism of a non-BCS nature which can stabilize a superconducting state in a *strongly repulsive* electronic system. By considering the two-dimensional Hubbard model with spatially modulated electron hoppings, we demonstrate how kinetic-energy frustration can lead to robust *d*-wave superconductivity at *arbitrarily* large on-site repulsion. This phenomenon should be observable in experiments using fermionic atoms, e.g. ⁴⁰K, in specially prepared optical lattices.

PACS numbers: 74.20.Mn, 71.10.Fd

Introduction.— One of the long-standing fundamental questions in condensed-matter physics is whether it is possible to realize a superconducting (SC) state in a system consisting only of electrons subject to a strong Coulomb repulsion, and if so, what is the minimal set of necessary physical assumptions. An early attempt to provide an answer was made by Kohn and Luttinger [1], who proposed a weak-coupling BCS-like mechanism. While their idea was never confirmed experimentally, there exist numerous *strongly* correlated systems whose SC behavior occurs without any obvious pairing glue, such as phonons, between the electrons. Examples are high- T_c cuprates and heavy fermion compounds. The current consensus is that superconductivity in these materials has an unconventional, i.e. non-BCS, character [2]. Understanding the microscopic origin of this intriguing phenomenon remains a challenge. Here we address the above question by performing a controlled derivation of the SC ground state (GS) for a *strongly-repulsive* Hubbard model with spatially modulated transfer integrals.

One possible way of stabilizing a Cooper pair condensate in a repulsive system is to introduce microscopic inhomogeneities. Indeed, the nanoscale spin and charge modulations, observed in scattering [3], ARPES [4] and STM [5] experiments, seem to be ubiquitous in high- T_c materials [6] and often accompany the emergence of the SC state. Theoretically it has been argued that these inhomogeneities are quite relevant for the superconductivity [7, 8] and, in fact, seem to assist the Cooper pairing. This was demonstrated in [7, 9] by using exact diagonalization of strongly interacting models in finite lattices. In Ref. 10 the authors studied the Hubbard model on a checkerboard lattice, composed of weakly coupled 2×2 plaquettes, and showed that the SC phase can be stabilized in a relatively narrow interval of the on-site repulsion U . Earlier, a similar problem was considered in [11]. Another ingredient, whose importance for superconductivity was largely overlooked, is the range of the transfer integrals beyond nearest-neighbors (NN). The next-NN (NNN) hopping, t' , was shown to enhance $d_{x^2-y^2}$ -like pairing correlations in the t - t' - J model on finite clusters [12]. Physically, its main qualitative effect is the possible

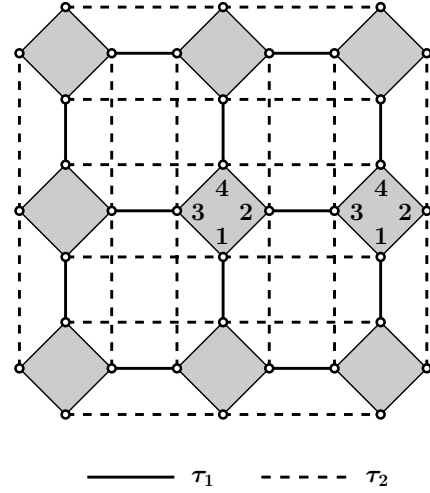


FIG. 1: The tetrahedral lattice topology. The interplaquette hopping amplitudes are: NN τ_1 (solid lines) and NNN τ_2 (dashed lines). We only consider the case $\tau_2 \leq \tau_1$.

frustration of the kinetic-energy term: the smallest closed paths in the lattice are triangles instead of squares.

In the present Letter we explicitly demonstrate how *local* kinetic-energy *frustration* can stabilize the SC state in a *strongly repulsive* two-dimensional Hubbard model. The lattice, on which the model is defined, is presented in Fig. 1. It consists of weakly-coupled tetrahedra, i.e. plaquettes with frustrated hoppings along the diagonals. We show that a $d_{x^2-y^2}$ -wave SC phase exists for *arbitrarily* strong repulsion U . In fact, the problem can be treated analytically in the strong-coupling regime.

Our motivation to study this system is not purely academic. Advances in experimental methods of preparation and manipulation of ultracold fermion atoms in optical lattices provide a controlled way of testing the above-mentioned theoretical ideas. For example, in recent experiments [13, 14] the observation of a Mott state with ⁴⁰K atoms was reported. Moreover, an experiment aimed to find *d*-wave superconductivity in a checkerboard Hubbard model was proposed in Ref. 15.

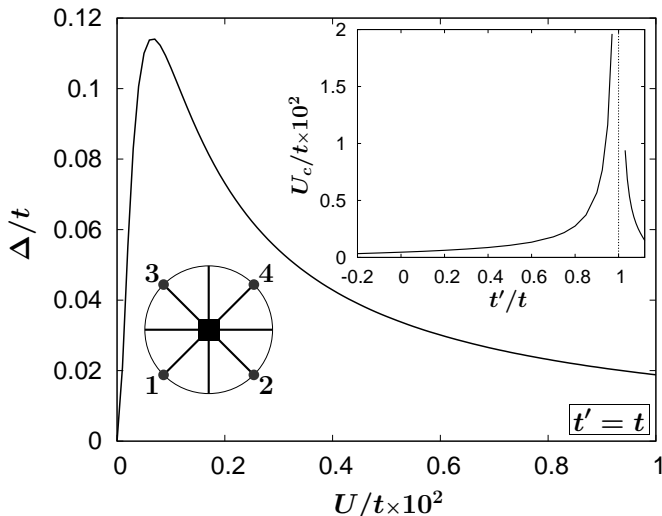


FIG. 2: Hole binding energy $\Delta(U)$. The asymptotic behavior is: $\Delta(U \gg t) \approx 2t^2/U$ and $\Delta(U \ll t) \approx U^2/32t$. Upper inset: critical value $U_c(t')$ [$\Delta(U_c) = 0$]. Lower inset: group C_{4v} . Numbers indicate plaquette vertices. The black square denotes four-fold axis C_4 , horizontal and vertical lines – primary symmetry planes σ_v , diagonals – secondary planes σ'_v .

Model. – Let us consider the repulsive Hubbard model:

$$H = - \sum_{\langle ij \rangle, \sigma} t_{ij} (c_{i\sigma}^\dagger c_{j\sigma} + \text{h.c.}) + U \sum_i n_{i\uparrow}^e n_{i\downarrow}^e, \quad (1)$$

defined on the lattice, Fig. 1, in terms of fermionic (creation) operators $c_{i\sigma}^\dagger$. Here $\langle ij \rangle$ denotes links connecting sites i and j , $\sigma = \{\uparrow, \downarrow\}$ is the electron spin, and $n_{i\sigma}^e = c_{i\sigma}^\dagger c_{i\sigma}$. The amplitudes t_{ij} take four possible values: (i) t for links $\langle 12 \rangle$, $\langle 13 \rangle$, $\langle 24 \rangle$ and $\langle 34 \rangle$; (ii) t' for the diagonals $\langle 14 \rangle$ and $\langle 23 \rangle$; (iii) τ_1 for NN links, connecting two plaquettes; (iv) τ_2 for NNN interplaquette links.

We will consider the case $\tau_{1,2} \ll t, t', U$, which allows for a controlled perturbative expansion of the Hamiltonian (1). To demonstrate the existence of a robust SC phase, we derive a low-energy effective model, accurate to second order in $\tau_{1,2}$. In general, this is doable only numerically. However, in the limit $t, t' \ll U$, we can keep only lowest-order terms in t_{ij}/U , and thus provide a closed form for the effective Hamiltonian (EH). The stability of the Cooper pair condensate can be tuned by changing the ratio t'/t . There is an “optimal” value of this ratio, which ensures a finite energy gap (hole binding energy) between the plaquette states with one and two holes, for all finite U .

Single-plaquette states. – The Hubbard Hamiltonian on a single plaquette can be diagonalized exactly [11] by using representations of the crystallographic group C_{4v} (see the lower inset in Fig. 2). As a result, we can determine the hole binding energy $\Delta = 2\epsilon_0(3) - \epsilon_0(2) - \epsilon_0(4)$, where $\epsilon_0(N_e)$ is the GS for a given number of electrons

N_e . Positive values of Δ correspond to binding of two holes. In general, Δ is positive only in a finite range of U . At some critical value $U_c(t')$, shown in the upper inset of Fig. 2, it changes sign and remains negative as $U \rightarrow \infty$. There is a special ratio, $t'/t = 1$, at which U_c diverges and Δ stays *positive* for any value of U (see the main panel of Fig. 2). This results from the maximal frustration of the single-hole kinetic energy. The GS energy for 4 electrons (zero holes), $\epsilon_0(4) \rightarrow 0$ for $U \rightarrow \infty$ because the particles cannot move. On the other hand, in this limit $\epsilon_0(2) = 2\epsilon_0(3)$, which means that there is no kinetic-energy gain for creating two holes on different plaquettes; i.e., the single-hole kinetic energy is optimally frustrated. The exchange interaction $J = 4t^2/U$, that appears for finite $t/U \ll 1$, leads to pairing ($\Delta > 0$) because the magnetic configuration of two plaquettes with one hole in each of them is more frustrated than the configuration with two holes in the same plaquette. This leads to a positive value of $\Delta = J/2$.

From now on we will only consider the maximally frustrated point $t'/t = 1$. Then, the symmetry group \mathcal{G} of the single-plaquette Hamiltonian is larger than C_{4v} (symmetry group for arbitrary t'/t), and contains all the independent permutations of any pair of vertices of the plaquette. This symmetry translates into a GS degeneracy at half-filling. There are two $SU(2)$ -singlet states: one transforming as the identity representation of C_{4v} , A_1 (s -wave), and the other – as B_1 ($d_{x^2-y^2}$ -wave) [16]. These states are connected by symmetry operations from the factor group \mathcal{G}/C_{4v} . The two-electron GS is also a singlet and belongs to the identity representation of \mathcal{G} . The $N_e = 3$ GS has $S = 1/2$ and is six-fold degenerate.

General expressions for these eigenstates are quite cumbersome. However, to the lowest order in t/U , we can consider only states without doubly occupied sites. Hence, we have the GS for $N_e = 2$: $|\Omega_2\rangle = (1/2\sqrt{3}) \sum_{\langle ij \rangle} s_{ij}^\dagger |0\rangle$ with the summation extended over all links of a plaquette; and for $N_e = 4$: $|\Omega_4^{s,d}\rangle = \mathcal{N}_{s,d} (s_{13}^\dagger s_{24}^\dagger \pm s_{12}^\dagger s_{34}^\dagger) |0\rangle$. In these expressions s_{ij}^\dagger is a singlet creation operator, $s_{ij}^\dagger = c_{i\uparrow}^\dagger c_{j\downarrow}^\dagger - c_{i\downarrow}^\dagger c_{j\uparrow}^\dagger$, $|0\rangle$ is the empty state and $\mathcal{N}_s = -1/2$, $\mathcal{N}_d = 1/2\sqrt{3}$. Finally, we introduce operators P_{ij} , which permute sites i and j . In the basis $\{|\Omega_4^s\rangle, |\Omega_4^d\rangle\}$, P_{12} and P_{13} have the form: $P_{12,13} = -\sigma^z/2 \pm \sqrt{3}\sigma^x/2$ with σ^α ($\alpha = x, z$) Pauli matrices. We will use this expression to determine symmetries of the effective model.

Effective low-energy model. – The low-energy spectrum of decoupled plaquettes has a gap Δ to single-hole ($N_e = 3$ on each plaquette) states. Here we consider the effect of finite hopping amplitudes $\tau_{1,2}$ by assuming that $0 \leq \tau_{1,2} \ll \Delta \sim t^2/U \ll t \ll U$. The second inequality allows us to treat interplaquette hoppings perturbatively. The fourth one allows us to exclude states with doubly occupied sites, i.e. use as a basis the states $|\Omega_2\rangle$ and $|\Omega_4^{s,d}\rangle$. Finally, the third inequality constrains the

choice of the virtual states: only states that belong to the $N_e = 3$ GS sextet contribute to lowest order. We will also assume that $\tau_2 \leq \tau_1$.

The second-order EH can be symbolically written as:

$$H_{\text{eff}} = \mathcal{P}^{(0)} H_\tau (1 - \mathcal{P}^{(0)}) \frac{1}{E_0 - H^{(0)}} (1 - \mathcal{P}^{(0)}) H_\tau \mathcal{P}^{(0)},$$

where $H^{(0)}$ describes a set of noninteracting plaquettes in (1), E_0 is its GS energy, H_τ denotes plaquette interactions, and $\mathcal{P}^{(0)}$ is a projector onto the subspace with $N_e = 2$ or 4 on each plaquette. Next, we associate the product of the two-electron plaquette GS with the vacuum: $|\text{vac}\rangle = \prod_x |\Omega_2\rangle_x$ and each member of the four-electron GS doublet on plaquette x – with a hard-core boson: $|\Omega_4^\alpha\rangle_x = b_{x\alpha}^\dagger |\Omega_2\rangle_x$, where $\alpha = s$ or d represents the pseudospin index. The algebra generated by $b_{x\sigma}$ was discussed in Ref. 17. Thus, the effective low-energy theory, given by H_{eff} , describes a system of two-flavor hard-core bosons, propagating in the coarse-grained plaquette lattice of Fig. 1. In terms of these boson operators we have:

$$H_{\text{eff}} = \sum_{\langle xy \rangle, \alpha\beta} t_{\alpha\beta}^{\text{eff}} (b_{x\alpha}^\dagger b_{y\beta} + b_{y\beta}^\dagger b_{x\alpha}) - \mu \sum_{x,\alpha} n_{x\alpha} + \quad (2)$$

$$+ \sum_{\langle xy \rangle, \alpha\beta} V_{\alpha\beta}^{\text{eff}} [(1 - n_x) b_{y\alpha}^\dagger b_{y\beta} + (1 - n_y) b_{x\alpha}^\dagger b_{x\beta}],$$

where $\langle xy \rangle$ denotes NN plaquettes, $t_{\alpha\beta}^{\text{eff}}$ are corresponding hopping amplitudes, $V_{\alpha\beta}^{\text{eff}}$ – density-density and local spin-flip interactions, $n_{x\alpha} = b_{x\alpha}^\dagger b_{x\alpha}$ and $n_x = n_{xs} + n_{xd}$, and μ is the chemical potential. Direct interactions between pseudospins, like Heisenberg terms, are not present to lowest order in Δ/t and t/U .

Some general properties of t^{eff} and V^{eff} can be established by symmetry arguments. First, the Hamiltonian (1) is invariant under reflections in the planes which include τ_1 links, e.g. the plane connecting sites 2 and 3 in Fig. 1. The states $|\Omega_2\rangle$ and $|\Omega_4^s\rangle$ are symmetric under this operation, while the d -wave state $|\Omega_4^d\rangle$ is antisymmetric. Consequently, the off-diagonal matrix elements of t_{sd}^{eff} and V_{sd}^{eff} vanish: $t_{\alpha\beta}^{\text{eff}} = t_{\alpha\alpha}^{\text{eff}} \delta_{\alpha\beta}$, $V_{\alpha\beta}^{\text{eff}} = V_{\alpha\alpha}^{\text{eff}} \delta_{\alpha\beta}$. This result is independent of the assumptions made regarding the relative magnitude of $\tau_{1,2}$, U and t .

Another observation concerns the diagonal elements of t^{eff} and V^{eff} in the special cases $\tau_2 = \tau_1$ and $\tau_2 = 0$. In the first case, we consider the two plaquettes with numbered sites, shown in Fig. 1, and perform simultaneous permutations of vertices $1 \leftrightarrow 2$ on the left plaquette and $1 \leftrightarrow 3$ on the right one. Each operation is a symmetry of the single-plaquette Hamiltonian. Their combination amounts to interchanging the τ_1 and τ_2 links, which is now a symmetry of the connecting Hamiltonian. Using the relation $P_{12,13} |\Omega_2\rangle = |\Omega_2\rangle$, it is easy to show that for $\tau_1 = \tau_2$: $t_{ss}^{\text{eff}} = -t_{dd}^{\text{eff}}$ and $V_{ss}^{\text{eff}} = V_{dd}^{\text{eff}}$. In the case $\tau_2 = 0$, when the plaquettes are connected by only one τ_1 link,

the second-order virtual hopping of an electron can only proceed through an intermediate state, whose energy is of order U . Therefore, in the approximation formulated above, t^{eff} must vanish. On the contrary, V^{eff} is not associated with the net electron transfer and remains finite.

In general, a direct calculation yields the precise form of the coefficients t^{eff} and V^{eff} :

$$t_{\alpha\beta}^{\text{eff}} = -(\tau_1^2/6\Delta) \text{diag}\{r_\tau(2r_\tau + 1), -3r_\tau\}; \quad (3)$$

$$V_{\alpha\beta}^{\text{eff}} = -(\tau_1^2/48\Delta) \text{diag}\{9 + 8r_\tau + 16r_\tau^2, 9 + 24r_\tau^2\}$$

with $r_\tau = \tau_2/\tau_1$. Clearly, in the two special cases, discussed above – $r_\tau = 1$ and 0 – the EH (2) becomes pseudospin symmetric. The second case is irrelevant for the purposes of studying the SC state, while the first one, $r_\tau = 1$, is quite instructive. Indeed, in this case we can use the Perron-Frobenius theorem to prove that there exists a pseudospin-polarized GS [18]. The Hamiltonian can then be written only in terms of spinless bosons, say b_{xd} , and maps onto the spin-1/2 XXZ model in a magnetic field μ , via the Matsubara-Matsuda transformation [19]. The phase diagram of this model contains Néel, canted XY-antiferromagnetic and fully polarized states that are immediately identified with the density-wave (DW), Bose-Einstein condensate (BEC) of Cooper pairs, and Mott phases, respectively. The DW and BEC states are separated by a 1st order quantum phase transition.

We do not expect the physics to change qualitatively for $0 < r_\tau < 1$. It is known that the usual mean-field approximation yields satisfactory results for $r_\tau = 1$ when compared to Monte-Carlo simulations [20]. Thus, we anticipate that the rest of the phase diagram, along the r_τ axis, can be described within a simple variational approach. We employ the method of [21], which includes short-range quantum fluctuations and, as a limit, contains the semiclassical spin-wave ansatz. The resulting phase diagram, obtained using 2×2 site clusters (in the plaquette lattice), is presented in Fig. 3. For any finite $0 < r_\tau < 1$ the system exhibits the same three phases, as in the case $r_\tau = 1$. The SC and DW phases are again separated by a 1st order transition. The transition between SC and Mott phases is 2nd order. In the Mott state there is exactly one boson per site; i.e., the electron filling is 1/2. In this phase the pseudospin polarization is undefined, as the Hamiltonian (2) becomes spin-independent. Interestingly, the DW phase is of an s -wave nature, due to the fact that the expectation value of the kinetic energy vanishes, while density-density interactions favor the s -wave pseudospin polarization.

The SC state has a $d_{x^2-y^2}$ -wave symmetry. The structure of the ‘‘Cooper pair’’ can be determined by observing that $b_d = \mathcal{D}/3 - (1/4)(s_{14} + s_{23})(\uparrow\uparrow\downarrow\downarrow - \uparrow\downarrow\uparrow\downarrow)$, where $\uparrow\uparrow = s_{13}^\dagger s_{24}^\dagger |0\rangle$, $\uparrow\downarrow = s_{12}^\dagger s_{34}^\dagger |0\rangle$ and $\mathcal{D} = s_{13} + s_{24} - s_{12} - s_{34}$ (see the lower inset of Fig. 2). Hence, despite the apparent complexity of the SC phase, it can still be characterized by a familiar d -wave order parame-

ter $\Delta_d = \langle \mathcal{D} \rangle$, shown in the inset of Fig. 3 for $r_\tau = 1$. As r_τ decreases, the height of the SC dome gradually diminishes and disappears at $r_\tau = 0$. Thus, for any $0 < r_\tau < 1$ there is an interval of μ where the SC phase is stabilized. This conclusion becomes rigorous in the dilute limit of particles or holes, by virtue of the inequality $|t_{dd}^{\text{eff}}| > |t_{ss}^{\text{eff}}|$, valid for $r_\tau < 1$ [see Eq. (3)].

Discussion.— Our phase diagram, Fig. 3, was obtained in the strong-coupling limit $U \gg t$, where one can derive the effective model of Eqs. (2), (3). The EH becomes increasingly complicated for intermediate couplings $U \sim t$, because of the large number of virtual transitions. In this regime, the existence of d -wave superconductivity in the nonfrustrated Hubbard model was argued in [10] based on a first-order EH, treated within a mean-field approximation, and in the weak-coupling regime $U \ll t$ in [22]. Therefore, we expect the SC phase to persist for $U \sim t$ in our frustrated case as well. However, regardless of the magnitude of U , the SC state is quite sensitive to the presence of longer-range repulsions. For instance, an interaction of the form $\sum V_{ij} n_i^e n_j^e$ with $V_{ij} = V$ for all links within the plaquette, will suppress the local hole binding if $V \geq V_c = 0.114t$. For $V < V_c$ the SC phase is stable only in a finite interval of U around $U \sim 7t$.

Our theory highlights the importance of the kinetic-energy frustration for stabilizing the SC state. Locally, pairing competes against the kinetic energy and can be increased by frustrating the latter. This principle guides the choice of the *elementary unit*, e.g., tetrahedron. The *connectivity* of the lattice, built from these blocks is another essential ingredient. Here we used the lattice of

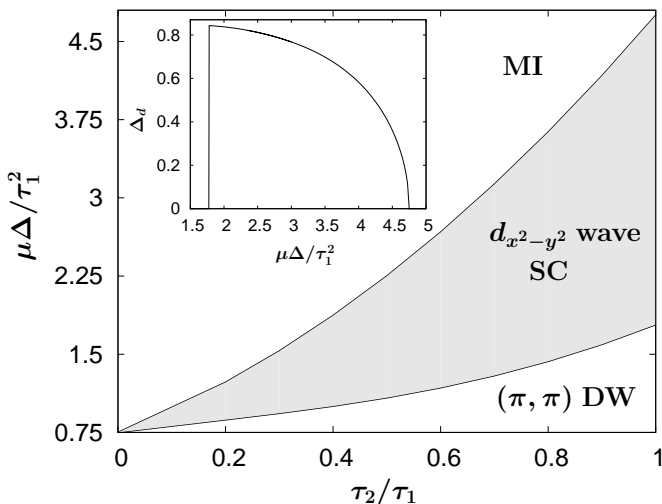


FIG. 3: Low-energy phase diagram of the Hubbard model Eq. (1). Phases are: s -wave density wave (DW) with wavevector (π, π) ; d -wave SC, which corresponds to a BEC of b_d ; Mott insulating (MI) phase with $\langle n_x \rangle = 1$. The DW – SC phase transition is 1st order; the SC – MI transition is 2nd order. The inset shows $\Delta_d \sim \langle b_{xd} \rangle$ for $r_\tau = 1$.

Fig. 1 to demonstrate the existence of the SC state in a physically transparent way. However, we also considered the usual checkerboard lattice [10]. In this case the relation between coefficients in the EH is such that the phase-separated state can suppress superconductivity in a certain region of the phase diagram. The importance of the lattice topology is further illustrated by the case $\tau_2 = 0$. Without the interplaquette hopping (3), the global phase coherence can be established only in higher orders in $1/U$, leading to a quite fragile SC state.

Finally, we believe that the lattice of Fig. 1 can be realized using ideas of Refs. 15, 23. Indeed, our effective strong-coupling model can be easily extended to the currently experimentally realizable regime $t'/t \lesssim 0.5$ under the condition $t \ll U < U_c$, which can still be fulfilled for $t'/t = 0.5$ because $U_c \approx 11t$ (see inset of Fig. 2). The resulting phase diagram is qualitatively the same as the one shown in Fig. 3. Thus, results of the present Letter can be tested in future cold atom experiments.

Acknowledgements.— LI acknowledges the hospitality of CNLS at LANL. CDB was supported by US DOE.

-
- [1] W. Kohn and J. M. Luttinger, Phys. Rev. Lett. **15**, 524 (1965).
 - [2] P. Monthoux, D. Pines, and G. G. Lonzarich, Nature **450**, 1177 (2007).
 - [3] J. M. Tranquada *et al.*, Nature **375**, 561 (1995).
 - [4] T. Valla *et al.*, Science **314**, 1914 (2006).
 - [5] W. D. Wise *et al.*, Nature Phys. **5**, 213 (2009).
 - [6] E. Dagotto, Science **309**, 257 (2005).
 - [7] J. Eroles *et al.*, Europhys. Lett. **50**, 540 (2000).
 - [8] S. A. Kivelson and E. Fradkin in *Treatise of High Temperature Superconductivity*, J. R. Schrieffer and J. Brooks eds. (Springer-Verlag, Berlin, 2007).
 - [9] W. F. Tsai *et al.*, Phys. Rev. **B77**, 214502 (2008).
 - [10] H. Yao, W. F. Tsai, and S. A. Kivelson, Phys. Rev. **B76**, 161104 (2007).
 - [11] A. F. Barabanov, L. A. Maksimov, and A. V. Mikheyenkoy, J. Phys.: Cond. Matter **1**, 10143 (1989).
 - [12] G. B. Martins *et al.*, Phys. Rev. **B64**, 180513 (2001).
 - [13] R. Jördens *et al.*, Nature **455**, 204 (2008).
 - [14] U. Schneider *et al.*, Science **322**, 1520 (2008).
 - [15] A. M. Rey *et al.*, Europhys. Lett. **87**, 60001 (2009).
 - [16] L. D. Landau and E. M. Lifshitz, *Quantum Mechanics* (Pergamon Press, Oxford, 1977).
 - [17] C. D. Batista, G. Ortiz, and J. E. Gubernatis, Phys. Rev. **B65**, 180402 (2002).
 - [18] A. Fledderjohann *et al.*, Eur. Phys. J. **B43**, 471 (2005).
 - [19] C. D. Batista and G. Ortiz, Adv. in Phys. **53**, 1 (2004).
 - [20] G. G. Batrouni and R. T. Scalettar, Phys. Rev. Lett. **84**, 1599 (2000).
 - [21] L. Isaev, G. Ortiz, and J. Dukelsky, Phys. Rev. **B79**, 024409 (2009).
 - [22] S. Raghu, S. A. Kivelson, and D. J. Scalapino, Phys. Rev. **B81**, 224505 (2010).
 - [23] L. Jiang *et al.*, Phys. Rev. A **79**, 022309 (2009).